Behavior of liquid plugs at bifurcations in a microfluidic tree network

Nadia Vertti-Quintero, Yu Song, Paul Manneville, and Charles N. Baroud

Articles you may be interested in

Wicking flow through microchannels
Phys. Fluids **23**, 122108 (2011); 10.1063/1.3671739

Asymmetry of red blood cell motions in a microchannel with a diverging and converging bifurcation
Biomicrofluidics **5**, 044120 (2011); 10.1063/1.3672689

Electrowetting on gold electrodes with microscopic three-dimensional structures for microfluidic devices
J. Appl. Phys. **104**, 064910 (2008); 10.1063/1.2976358

Effect of bifurcation angle in tree-shaped microchannel networks
J. Appl. Phys. **102**, 073530 (2007); 10.1063/1.2794379

Microfluidic model of bubble lodging in microvessel bifurcations
Appl. Phys. Lett. **89**, 244103 (2006); 10.1063/1.2402898

Behavior of liquid plugs at bifurcations in a microfluidic tree network

Nadia Vertti-Quintero, Yu Song, Paul Manneville,[a)] and Charles N. Baroud
Hydrodynamics Laboratory, CNRS UMR7646, École Polytechnique, 91128 Palaiseau, France

Flows in complex geometries, such as porous media or biological networks, often contain plugs of liquid flowing within air bubbles. These flows can be modeled in microfluidic devices in which the geometric complexity is well defined and controlled. We study the flow of wetting liquid plugs in a bifurcating network of micro-channels. In particular, we focus on the process by which the plugs divide as they pass each bifurcation. The key events are identified, corresponding to large modifications of the interface curvature, the formation of new interfaces, or the division of a single interface into two new ones. The timing of the different events and the amplitude of the curvature variations are analyzed in view of the design of an event-driven model of flow in branching micro-networks. They are found to collapse onto a master curve dictated by the network geometry. © *2012 American Institute of Physics*. [http://dx.doi.org/10.1063/1.4739072]

I. CONTEXT

A detailed understanding of two-phase dynamics in networks of micro-channels is of interest in many applications,[1–3] including porous media imbibition or the flow of physiological fluids for example in the lung[4,5] or in the micro-circulation.[6] At length scales below approximately 2 mm, inertia is most often irrelevant (small Reynolds and Weber numbers) and the dynamics is controlled by viscous effects in the bulk and surface-tension effects at the interfaces.[7] While motion of fluid plugs or bubbles along straight portions has found a satisfactory description,[8,9] complications arise at channel junctions where they divide and possibly break.[10]

Here, we focus on a binary branched network that was originally designed to study pulmonary flow in an intermediate range of bronchial tubes in the lung for which microfluidic modeling is relevant.[11] More specifically, we scrutinize the dynamics of liquid plugs at successive bifurcations in two steps, first by identifying key events and then by studying the timing of these events in order to point out similarity in the dynamics. Our aim is to find the ingredients of an event-driven numerical model applicable, e.g., to the therapy of some lung pathologies.[12,13]

In contrast with previous work that looked at drops or bubbles in bifurcating micro-channels and focused on the division of the non-wetting phase,[6,14,15] we concentrate our attention on the behavior of the wetting phase. The plugs that we observe, being subjected to dominant wetting effects, therefore always split when passing the bifurcation. On the contrary, the non-wetting phase can pass the bifurcation without dividing if the viscous forces from the extensional flow, which pulls the drop apart, are too weak. This motivates our focus on the details of the behavior of interfaces as they pass the bifurcations, and not only the final state that is reached.

II. SETTING

Our hierarchical binary network is depicted in Figure 1. Micro-channels are prepared by soft lithography techniques in a polydimethysiloxane (PDMS) block. From generation to

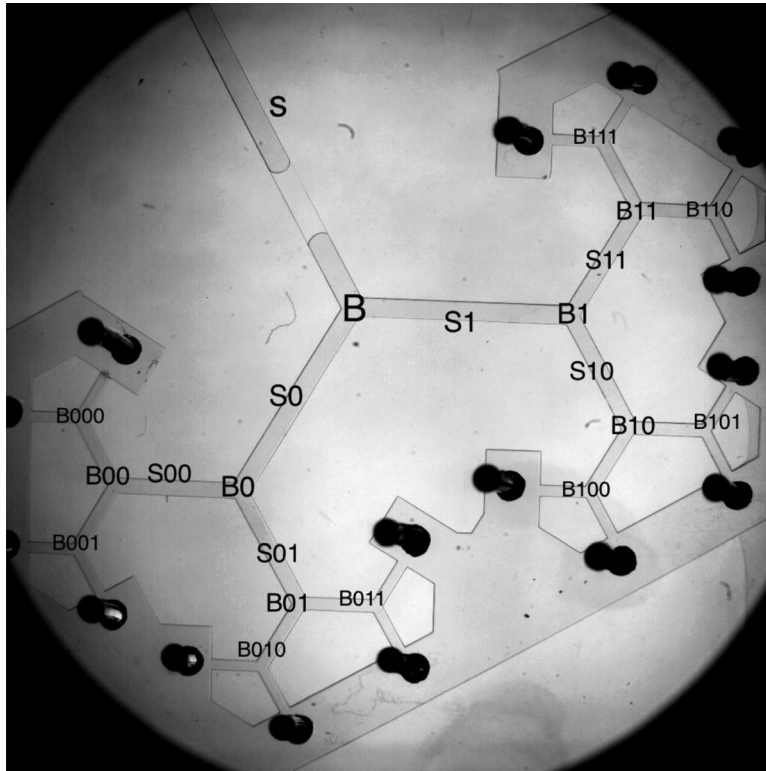a)paul.manneville@polytechnique.edu.

6, 034105-1

FIG. 1. The binary structure of the network is reflected in the labeling of the channels (S) and bifurcations (B). In the experiments reported here, a constant pressure head ΔP_{dr} is applied between the entrance and the exits. The shape and position of a liquid plug is detected thanks to the image contrast, with liquid plugs appearing transparent and air in light gray. The dynamics of the plugs in the network is deduced from the examination of image time-series. The experiment with $\Delta P_{dr} = 250\,\text{Pa}$ is displayed at 6 frames per second, i.e., $10\times$ slowing-down, in the attached movie (enhanced online). [URL: http://dx.doi.org/10.1063/1.4739072.1]

generation, the widths of the channels vary as $w_i = \rho w_{i-1}$ where i is the generation number, with $\rho = 0.83$, $w_0 = 720\mu m$ being the width of the root channel. The height of the channels is $h = 50\mu m$ uniformly, and the branching angle is $120°$.[16]

Droplets of perfluorodecalin (PFD) with viscosity $\eta = 5 \times 10^{-3}\,\text{Pa s}$ and surface tension $\gamma = 20 \times 10^{-3}\,\text{N/m}$ are instilled into the network initially filled with air. We call them plugs since they occupy the full section of the channels. They are driven by a constant pressure head ΔP_{dr} applied between the entrance of the network and its outlets. In the experiment analyzed below, $\Delta P_{dr} = 250\,\text{Pa}$. Their motion along a straight segment is well understood as the result of a competition between capillary forces and viscous losses. For small capillary numbers $\text{Ca} = \eta U/\gamma$, viz. $\text{Ca} < 10^{-2}$, one gets $\Delta P_{dr} = F(w)\ell\,U + G(w)U^{2/3}$, where ℓ is the length of the liquid plug, U its speed, F and G two known functions of the local width w of the channel along which it moves.[10] This formula assumes $h \ll w \ll \ell$ and corrections are needed when these inequalities are violated, which will be the case sufficiently deep in the network since the channel widths decrease at a rate $\rho = 0.83$. Owing to volume conservation, the plug lengths decrease at a rate $1/2\rho = 0.60$ from about $2\,\text{mm}$ in the root channel. In practice, due to the fluid film left behind them as they move, liquid plugs see their length decrease a bit faster, in line with results to be presented in Fig. 8.

Experiments are recorded with a high speed camera (Photron Fastcam, 1024 PCI) through a stereomicroscope at $0.7\times$ magnification. The resolution of the camera is 1024×1024 pixels, which yields 1 pixel for 24.8 μm. Images are taken at rates varying from 30 to 125 images per second, according to the driving conditions, thus ensuring that the plug positions can be traced with a sufficient resolution. The movies are then stored as individual tiff images, which are then analyzed

using the IMAGEJ processing software or MATLAB, by manually locating the position of the rear interface at each frame. The movie most specifically used in the following is linked to Figure 1.

Here, extending our previous work which was limited to the global behavior of the flow in the network,[11,17] we focus on the motion of plugs through bifurcations by examining the time it takes for a plug to cross the bifurcation at different levels in the hierarchical network. We consider the behavior of a plug at the first bifurcation in Sec. III A, and next how its daughters evolve through the subsequent bifurcations in Sec. III B, showing the dominant role of geometric similarity in view of the construction of a general evolution model (Sec. V).

III. RESULTS

A. Crossing the first bifurcation: Events, stages, and timings

Channels and bifurcations are labelled according to their position using a pseudo-binary code (Fig. 1): The entrance channel S splits into two channels S0 and S1 at bifurcation B. S0 splits into S00 and S01 at B0 and S1 into S10 and S11 at B1, etc. We first consider a plug passing through bifurcation B (Fig. 2).
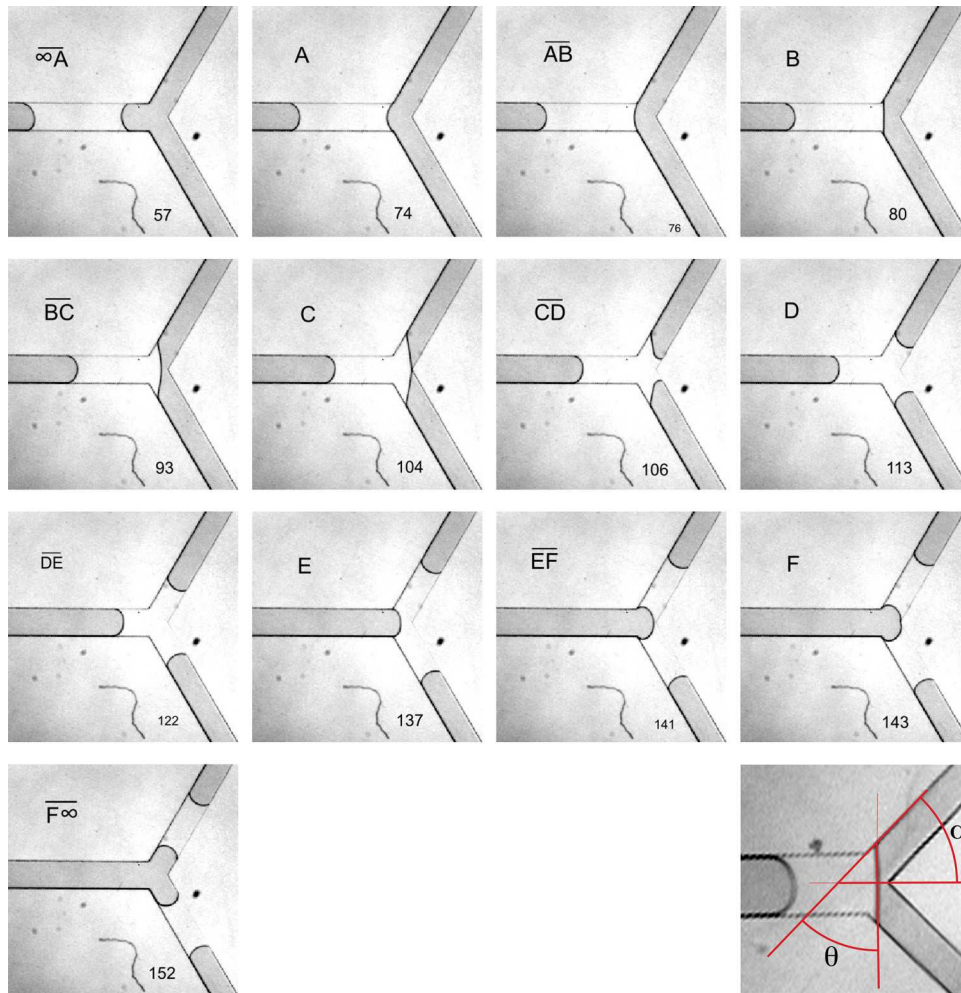

FIG. 2. Long plug crossing the first bifurcation: Stage $\overline{\infty A}$, frame #57. Event A, frame #74. Stage $\overline{AB}$, frame #76. Event B, frame #80. Stage $\overline{BC}$, frame #93. Event C, frame #104. Stage $\overline{CD}$, frame #106. Event D, frame #113. Stage $\overline{DE}$, frame #122. Event E, frame #137. Stage $\overline{EF}$, frame #141. Event F, frame #143. Stage $\overline{F\infty}$, frame #152. Images are captured at 60 frames per second. See text for details. Bottom-right: Illustration of the condition on contact angle θ and branching half-angle α that controls the sign of the interface curvature during stage $\overline{BC}$; when $\alpha = 45°$, the curvature is nearly zero.

Key events correspond to marked changes in the shapes of the plugs, especially the number of air-liquid interfaces and their curvatures. Before entering the bifurcation, stage $\overline{\infty A}$, the front and rear contact angles are about 40° and 30°, respectively. Event A corresponds to the front interface reaching the corner of the bifurcation. During stage $\overline{AB}$, the contact point is pinned at the corner and the curvature of the interface decreases progressively. Event B takes place when the contact line starts to move along the daughter channels S0 and S1. An orientation flip of the interface is associated with this de-pinning while the direction of daughter channels now serves as the reference for the contact-angle. The plug continues to advance during stage $\overline{BC}$ until event C when the front interface touches the corner of opposite wall. The variation of the curvature during this stage depends on the precise value of the contact angle θ and the bifurcation angle 2α (see bottom-right image of Fig. 2). If θ is smaller than $\frac{1}{2}\pi - \alpha$, the curvature of the front interface keeps the same sign during both stages. For our $(2\pi/3)$-bifurcation, it goes through zero and changes signs. This has, however, no qualitative consequences on the monotonic progression of the interface.

Event C leads to two front interfaces being formed, one in each daughter channel. Stage $\overline{CD}$ is just a reshaping of the newly formed front interfaces in order to minimize curvature. It ends when the interfaces have reached uniformly curved shapes. The corresponding event named D is not precisely defined but it is just a step in the evolution of the plug which, during stage $\overline{DE}$, continues to advance in branches S0 and S1 while completing its withdrawal from branch S. Event E is when the rear interface reaches the bifurcation and the reference direction for the receding contact angle flips from that of the mother channel to that of the daughter channels. The rear interface continues to advance during stage $\overline{EF}$ until it reaches the opposite corner, marking the second crucial event named F, when two independent plugs are formed and advance, moving along the daughter channels (stage $\overline{F\infty}$).

Bifurcations at higher levels will be considered later. Events C and F each correspond to important topological changes of the plug considered: At C, the front interface is forked into two, independent of the position of the rear interface which can still be in the mother channel or already in the bifurcation area depending on the plug length. Event E identified from a process taking place at the rear interface can therefore happen before event D which is related to a property of the two newborn front interfaces (see Fig. 3). Event F marks the birth of two plugs out of one. Events C and F are always present except when the plug is very short, in which case there is not enough liquid for two daughter plugs, the liquid bridge breaks and the channels are left open. The limit size of the plug that will cross a given bifurcation without breaking can be obtained mainly from a geometrical argument, up to a small correction function of the capillary number which controls the front contact angle.[10]

Figure 4 (top) displays the position in time of the rear interface of a liquid plug as it crosses bifurcation B, corresponding to the images in Figure 2. The slope of the curve directly gives the speed of the plug shown in Fig. 4 (bottom). It can be seen that the plug enters the
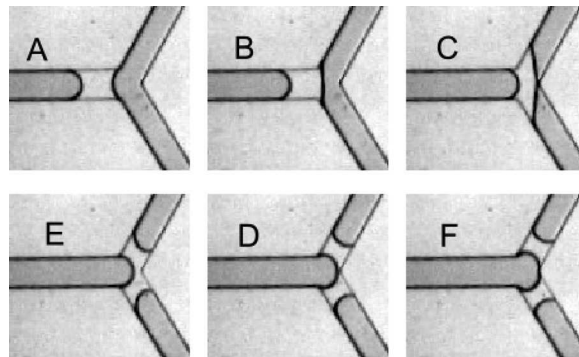

FIG. 3. Crossing of a plug at bifurcation B011 (see Fig. 1): Event A, frame #376; B, frame #379; C, frame #390; E, frame #392; D, frame #393; F, frame #394. When the plug is short, event E (rear interface reaching the corner) occurs before event D (end of front interface reshaping).
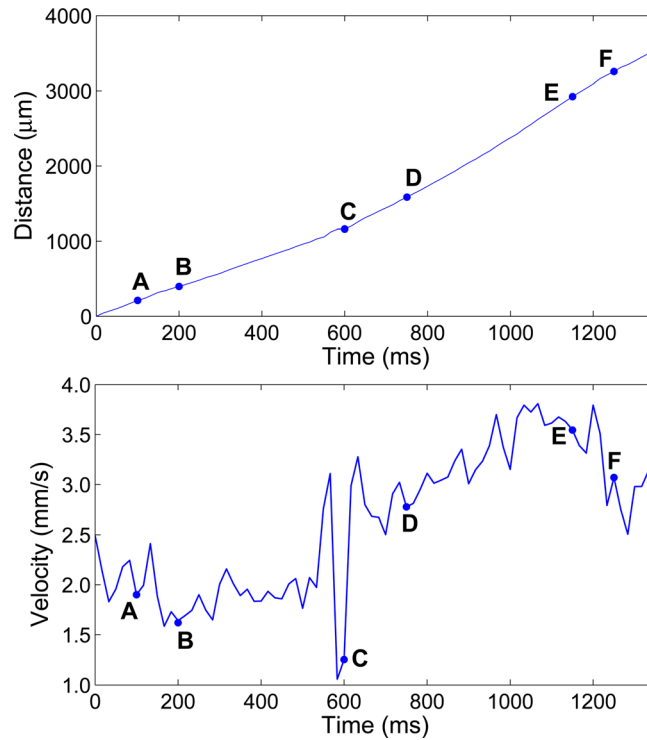
FIG. 4. Abscissa (top) and speed (bottom) of the rear interface along the channel as a function of time at bifurcation B, positioning events pointed out in Figure 2. The origin of distances is arbitrary.

bifurcation with some initial speed ($\overline{\infty A}$), first slows down ($\overline{AB} + \overline{BC}$), next accelerates ($\overline{CD} + \overline{DE}$), and slows down again ($\overline{EF}$) to reach a new speed ($\overline{F\infty}$). The large speed variations around events C and F are clearly related to the large reshaping experienced by the interfaces during the corresponding events.

The overall behavior during the bifurcation crossing can be understood from surface tension effects estimated through interface curvature measurements,[16,17] while the viscous part is less easily grasped than in the case of a straight channel.[10] The contribution of capillarity ΔP_{cap} to the driving pressure difference is then obtained from the Young–Laplace relation by taking for granted that the contribution from the curvature of the interface in the normal direction is essentially constant ($\propto 1/h$) and measuring interface curvatures in the plane of the network only using IMAGEJ. Capillary pressure variations estimated as the plug crosses bifurcation B are shown in Figure 5, where the different events and stages are easily identified. In particular, the
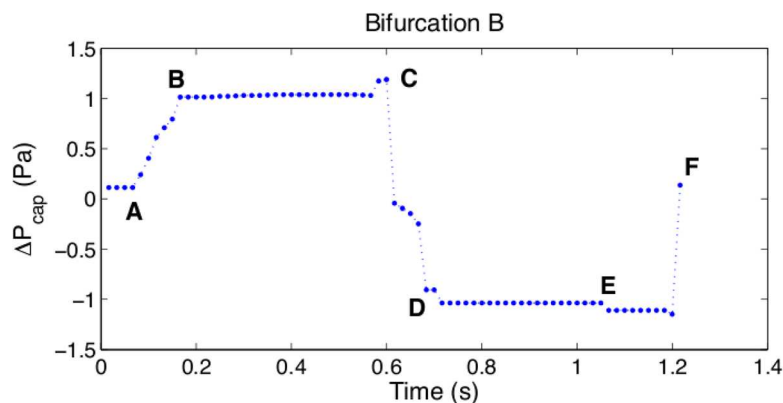

FIG. 5. Capillary contribution to pressure variations estimated from interface curvatures at the crossing of bifurcation B.

steep growth during stage $\overline{AB}$ clearly corresponds to the rapid decrease of curvature of the front interface, associated with a slight slowing down of the plug. On the other hand, the strong decrease to negative values beyond event C is caused by the suction induced by the sudden large curvature increase of the interfaces entering the daughter channels, which also corresponds to the acceleration observed in Figure 4. The slight overpressure observed during stages $\overline{\infty A}$ and $\overline{F\infty}$, at the very origin of the plug's motion, is computed from the curvature difference induced by the contact-angle imbalance between advancing and receding interfaces.

B. Subsequent bifurcations

As seen in Figure 6, the positions of the rear interfaces of plugs when they cross the second and third bifurcations follow trends similar to what is observed at the first bifurcation (Fig. 4), though on shorter and shorter time scales and with slightly different timings in the different branches. Timing differences can obviously be attributed to experimental imperfections, geometrical (network preparation), physicochemical (inhomogeneous mixing of the PDMS prior to polymerization), or dynamical (unequal division of plugs at a bifurcation): the deeper the network, the larger the impact.

As to the time scales, in Figure 7 (top) we display the capillary pressure difference ΔP_{cap} (estimated from interface curvatures as in Figure 5) versus time for three successive crossings, bifurcations B, B0 and B1, and B00 to B11. It is immediately seen that the time needed to cross a bifurcation decreases when the level increases. We can attribute this feature to a dominant effect of the viscous dissipation at these small scales itself related to the length of the liquid plugs. On the other hand, we get from geometrical considerations that pressure differences should increase as $1/\rho = 1.2$ from one level to the next, while the crossing times should decrease as $1/2\rho = 0.6$, which is the scale factor for the plug lengths. Rescaling pressure and
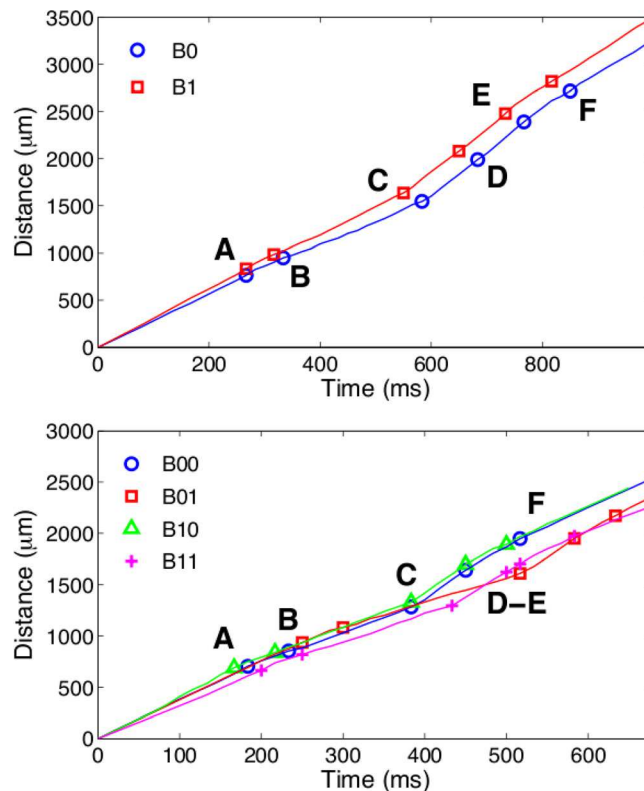

FIG. 6. Position of the rear interface as a function of time for higher level bifurcations. Top: bifurcations B0 and B1. Bottom: bifurcations B00, B01, B10, and B11.
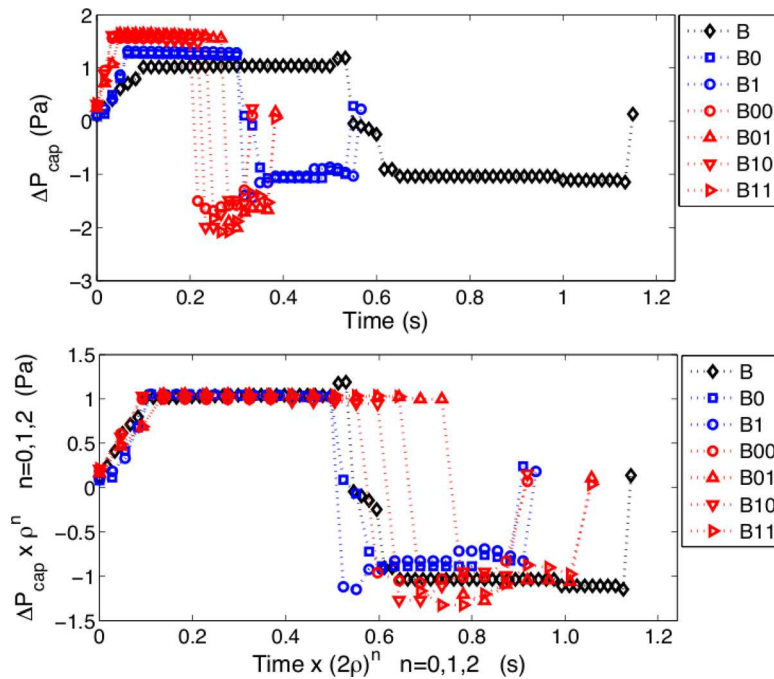
FIG. 7. Capillary pressure difference as function of time for different bifurcation levels. Top: raw data. Bottom: rescaled data.

times accordingly yield Figure 7 (bottom), where very good agreement is seen for pressures, while some dispersion is observed for times.

Events C and F are always marked by abrupt, hence easily detectable variations. The time dispersion is then mostly due to delays in the de-pinning of the interface at B or E, which induces fluctuations in the duration of stages $\overline{BC}$ and $\overline{DE}$ during which no important curvature rearrangements occur while the plug is translating at nearly constant pressure head. Experiments at lower (higher) driving pressure, $\Delta P_{dr} = 150 \, \text{Pa}$ ($\Delta P_{dr} = 400 \, \text{Pa}$ and $500 \, \text{Pa}$) support this interpretation. Dispersion is indeed much smaller at high pressure when defects are not strong enough to withstand the flow of plugs which therefore experience weaker pinning at corners. On the other hand, dispersion at low pressure is much larger with delays randomly introduced at the successive bifurcations.

As already mentioned, the dynamics of plugs has two facets, capillary and viscous. Considering viscosity effects, we may expect that friction, which is proportional to the surface wetted by the plugs, be proportional to their lengths, not only when they travel along a straight channel portion but also when they cross a bifurcation. This is indeed what happens, as shown in Figure 8
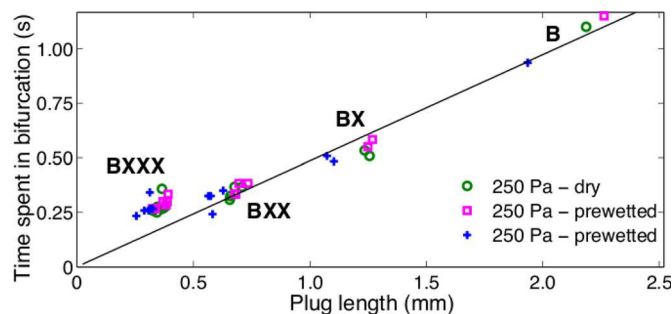

FIG. 8. Time difference between events F and A as a function of the length of entering plug for bifurcations B to BXXX, where X stands for 0 or 1.

which displays crossing times as functions of the plug lengths for three experiments performed under the same pressure head, starting with three slightly different initial lengths and different wetting conditions: either in pre-wetted networks as above or, on the contrary, in channels appropriately dried by blowing air into them before the start of the experiment. It can be observed that, from one bifurcation to the next, the length ratios are of the order of 0.55 instead of 0.60, which would be expected from geometrical considerations. This discrepancy is due to the volume of fluid lost by the plugs which, when traveling, leave a film of fluid along the walls of the channels. It is also noticed that small plugs take a longer time to cross the bifurcation than what is expected from strict proportionality to the length. The latter indeed should hold only for $h \ll w \ll \ell$ but additional dissipation is the consequence of non-negligible velocity gradients in the transverse direction ($w \ggg h$) and in the streamwise direction ($\ell \ggg w$) due to fluid recirculation within the shortest plugs. The fact that there is little dependence on the wetting conditions suggests that the dynamical contribution of capillarity at the front interface is a small correction to what the geometry-induced curvature generates.

IV. DISCUSSION

Restricted to what happens at bifurcations, the analysis presented here mostly takes into account the interplay between capillarity and geometry, while giving viscous effects a passive role. When a plug is flowing through a straight channel, there is no significant geometric forcing term due to curvature difference at the front and rear menisci ($\Delta P_{\text{geom}} \approx 0$): In the formula recalled earlier[10] (Sec. II), the nonlinear contribution just accounts for a residue of dynamical origin describing the viscous-capillary balance near the contact line.[18] Here, on the contrary, the deformations of the interfaces and the pressure differences they generate from curvature imbalance are essential, i.e., zeroth-order effects corrected for contributions of dynamical origin at next order. The dynamics of plug division through a bifurcation is then expected to result mainly from balancing the driving pressure by a geometric capillary pressure contribution and viscous losses.

We have seen that the crossing of the bifurcation involves stages of slow evolution and events of fast reorganization. In order to support the standpoint expressed above, it remains to show that we can disregard the brief flow reconfiguration phase that occurs around what we have called the crucial events, namely events C and F. A simple dimensional argument makes the point: Let us consider the flow of a plug through one of the abrupt width changes attached to these events, say from w to $w + \Delta w$. The geometric part of pressure head is due to the Young-Laplace law, that is $\Delta P_{\text{geom}} \sim \gamma/\Delta w \sim \gamma/w$, where symbol "$\sim$" means order of magnitude scaling, and the second estimate stems from the fact that we are interested in $\Delta w = (1 - \rho)w \propto w$. The fluid reconfiguration is resisted by viscous stresses generated by gradients of the accompanying velocity field V_{reorg}.

Since most of the viscous losses are due to velocity variations over the smallest dimension of the channel, its height h, these stresses can be written dimensionally as $\sigma_{\text{reorg}} \sim \eta V_{\text{reorg}}/h$. The amplitude of V_{reorg} is then obtained from $\Delta P_{\text{geom}} \sim \sigma_{\text{reorg}}$, hence $V_{\text{reorg}} \sim \gamma h/\eta w$. On the other hand, we are only interested in the result of this reorganization at scale w, which allows us to introduce a time scale $\tau_{\text{reorg}} \sim w/V_{\text{reorg}} = w^2 \eta/\gamma h$. By inserting typical values for our experimental conditions, we obtain $\tau_{\text{reorg}} \simeq 10^{-3}$ s. This is much shorter than the time needed to pass the bifurcation, which depends on the amount of fluid (length of the plug). For bifurcation B in the case discussed above (Fig. 4), $\tau_{\text{crossing}} \sim 1$ s. Notice that the ratio $\tau_{\text{reorg}}/\tau_{\text{crossing}}$ with $\tau_{\text{crossing}} \sim \ell/U$, where ℓ is the length of the plug is—apart from factors ℓ/w and w/h which are of order one in the experimental range of interest—nothing but an estimate of the capillary number, known to be small. All this means that a detailed description of the flow reorganization may be avoided and that the fluid in a plug adjusts almost immediately to any shape change. Therefore, the viscous effects only determine the slow part of motion, i.e., the passage of the plug through the bifurcation.

In order to construct a model of the plug's dynamics in the bifurcation, we must relate the driving pressure ΔP_{dr} to the positions of the front and rear interfaces $\Delta P_{\text{geom}}^{(i)}(x^{\text{f}}, x^{\text{r}})$ and to a

term that depends on the fluid properties. By comparison with the case of the plug advancing in a straight channel,[10] at lowest order we will get expressions in the form: $\Delta P_{\mathrm{dr}} = F^{(i)}(x^{\mathrm{f}}, x^{\mathrm{r}})U + \Delta P_{\mathrm{geom}}^{(i)}(x^{\mathrm{f}}, x^{\mathrm{r}})$, where $x^{\mathrm{f,r}}$ are the position of the front and rear interfaces, $U = \frac{\mathrm{d}}{\mathrm{d}t}x^{\mathrm{r}}$ and $\ell = \ell(x^{\mathrm{f}}, x^{\mathrm{r}})$. Here, superscript ($i$) indicates whether one considers the front interface during stages $\overline{\mathrm{AB}} + \overline{\mathrm{BC}}$ (one front interface) or $\overline{\mathrm{CD}} + \overline{\mathrm{DE}} + \overline{\mathrm{EF}}$ (two front interfaces), with possible refinement to treat stage $\overline{\mathrm{EF}}$ separately. The tedious task of finding functions $F^{(i)}$, $\Delta P_{\mathrm{geom}}^{(i)}$, and ℓ from geometrical considerations expressing volume conservation given the position $x^{\mathrm{f,r}}$ of the interfaces has, however, been left outside the scope of this exploratory work.

It should be noted that when the applied pressure head is too small, the plugs may not propagate through the network but stay blocked at some bifurcation level. This is due to the existence of a threshold to be overcome, again of capillary and geometric origin, that increases with the generation number.[16,17] In our experiment, this happens for $\Delta P_{\mathrm{dr}} \lesssim 150$. In contrast, when ΔP_{dr} is much larger, the plugs go faster and leave a thick film behind them.[9] They shorten and can rupture in one or both daughter channels at some level, a situation observed for $\Delta P_{\mathrm{dr}} \gtrsim 500\,\mathrm{Pa}$. When a plug ruptures, one or several channels get open from entrance to exit, offering a by-pass to the air that can no longer push the remaining plugs. Our findings are, therefore, valid for a limited set of generations in a certain range of pressures, but the similarity that has been pointed out remains of interest since, in the general case, these conditions can be met in some part of a large network.

In comparing with plug divisions in pulmonary airways, the mechanisms identified here shed some light on the flows that may take place *in vivo*. Although the geometry is different in the lung, capillary effects should still equilibrate with the tube geometry and thus affect the motion through a bifurcation through curvature changes as long as the capillary number is low, which is the case in distal airways. The model would, however, need to be improved to account for the circular shape of the bronchial tubes and, more importantly, for additional effects due to the lung's elasticity and deformability, or to the presence of surfactants, in order to better approach the pulmonary dynamics.[5]

V. TOWARDS AN EVENT-DRIVEN MODEL

In view of applications, it seems valuable to try to develop simplified but predictive models of plug dynamics in branched networks, as an alternative to much more demanding direct simulations. The kinematics of plugs in the straight segments of the network can be computed[10] and appropriate corrections for plug-length and lubrication effects can be included.[19] Fluid film deposition by the moving plugs can also be accounted for when several of them are successively introduced in the network.[20] Things become more delicate when bifurcations enter into play.

Our previous modeling attempts treated bifurcation crossings in a quasi-static way.[11,17] To improve over this limitation, we have tried to identify key events and their timing. Whatever the length of the plug entering a bifurcation, two events appear critical on topological grounds, when the front interface is forked into two (event C) and when the two daughter plugs effectively separate (event F). Above, we have alluded to the difficulty to extend the formula governing the dynamics of plugs in straight segments[10] to the case of crossings. We have, however, noticed that a simple geometrical argument was sufficient to rescale high level bifurcations onto low level ones, up to uncertainties linked to experimental imperfections (Fig. 7). In the same way, the duration of a crossing was found essentially proportional to the length of the plug with easily understandable corrections for short plugs (Fig. 8).

In practice, we are interested in the dynamics of multiple plugs scattered in different regions of the network. The events that we have identified here are generic and can serve as flags for the evolution of one plug among the others. Accordingly, the results presented here for timings between our key events can be combined with the models for motion in straight segments[10] and branched networks[11] to build an event-driven simulation. This can also be complemented by including the interaction between successive plugs *via* film deposition up to plug rupture.[20] Such a model would be useful to predict transport in hierarchical branched networks

such as the intermediate range of bronchial tubes in the lung, for instance, to predict the distribution of therapeutic drugs.[12]

[1]H. A. Stone, A. D. Strook, and A. Ajdari, "Engineering flows in small devices: Microfluidics toward a lab-on-a-chip," Annu. Rev. Fluid Mech. **36**, 381–411 (2004).

[2]W. Engl, M. Roche, A. Colin, P. Panizza, and A. Ajdari, "Droplet traffic at a simple junction at low capillary numbers," Phys. Rev. Lett. **95**, 208304 (2005).

[3]P. Parthiban and S. A. Khan, "Filtering microfluidic bubble trains at a symmetric junction," Lab Chip, **12**, 582–588 (2012).

[4]J. B. Grotberg, "Pulmonary flow and transport phenomena," Annu. Rev. Fluid Mech. **26**, 529–571 (1994).

[5]J. B. Grotberg, "Respiratory fluid dynamics," Phys. Fluids **23**, 021301 (2011).

[6]A. J. Calderón, Y. S. Heo, D. Huh, N. Futai, S. Takayama, J. B. Fowlkes, and J. L. Bull, "Microfluidic model of bubble lodging in microvessel bifurcations," Appl. Phys. Lett. **89**, 244103 (2006).

[7]C. N. Baroud, F. Gallaire, and R. Dangla, "Dynamics of microfluidic droplets," Lab Chip **10**, 2032–2045 (2010).

[8]L. W. Schwartz, H. M. Princen, and A. D. Kiss, "On the motion of bubbles in capillary tubes," J. Fluid Mech. **172**, 259–275 (1986).

[9]A. de Lózar, A. L. Hazel, and A. Juel, "Scaling properties of coating flows in rectangular channels," Phys. Rev. Lett. **99**, 234501 (2007).

[10]C. P. Ody, C. N. Baroud, and E. de Langre, "Transport of wetting liquid plugs in bifurcating microfluidic channels," J. Colloid Interface Sci. **308**, 231–238 (2007).

[11]Y. Song, M. Baudoin, P. Manneville, and C. N. Baroud, "The air-liquid flow in a microfluidic airway tree," Med. Eng. Phys. **33**, 849–856 (2011).

[12]W. A. Engle and the Committee on Fetus and Newborn, "Surfactant-replacement therapy for respiratory distress in the preterm and term neonate," Pediatrics **121**, 419–432 (2008).

[13]K. J. Cassidy, J. L. Bull, M. R. Glucksberg, C. A. Dawson, S. T. Haworth, R. Hirschl, N. Gavriely, and J. B. Grotberg, "A rat lung model of instilled liquid transport in the pulmonary airways," J. Appl. Physiol. **90**, 1955–1967 (2001).

[14]D. R. Link, S. L. Anna, D. A. Weitz, and H. A. Stone, "Geometrically mediated breakup of drops in microfluidic devices," Phys. Rev. Lett. **92**, 054503 (2004).

[15]L. Ménétrier-Deremble and P. Tabeling, "Droplet breakup in microfluidic junctions of arbitrary angles," Phys. Rev. E **74**, 035303 (2006).

[16]Y. Song, "Evolution of two-phase flow in networks of branching micro-channels," Ph.D. dissertation (École Polytechnique, 2010).

[17]Y. Song, P. Manneville, and C. N. Baroud, "Local interactions and the global organization of a two-phase flow in a branching tree," Phys. Rev. Lett. **105**, 134501 (2010).

[18]J. Bico and D. Quéré, "Falling slugs," J. Colloid Interface Sci. **243**, 262–264 (2001).

[19]H. Fujioka, S. Takayama, and J. B. Grotberg, "Unsteady propagation of a liquid plug in a liquid-lined straight tube," Phys. Fluids **20**, 062104 (2008).

[20]M. Baudoin, Y. Song, P. Manneville, and C. N. Baroud, "Airway re-opening through catastrophic events in a hierarchical network," Proc. Natl. Acad. Sci. U.S.A. (submitted).